

- [6] LIN, C. S., MOULTON, R. W. and PUTNAM, G. L., *Ind. Eng. Chem.*, **45**, 636 (1954).
- [7] DAVIES, C. N., *Aerosol Sci.*, **1**, 393 (1966).
- [8] LAWRENCE, W. R. and HUANG, A. B., «A. I. A. A. 10th Aerospace Sci. Meeting», A. I. A. A. Paper no. 72-81, San Diego, California, 1972.
- [9] BEAL, S. K., *Nucl. Sci. Eng.*, **40** (1970).
- [10] LEVICH, V. E., «Physicochemical Hydrodynamics», Prentice Hall, New Jersey, 1962, p. 155.
- [11] WELLS, A. C. and CHAMBERLAIN, A. C., *Brit. J. Appl. Phys.*, **18**, 1793 (1967).
- [12] OWEN, P. R., *Intern. J. Air Water Pollution*, **3**, 8, 50 (1960).
- [13] MONTGOMERY, T. L. and CORN, M., *Aerosol Sci.*, **1**, 185 (1970).
- [14] SEHMEI, G. A., *J. Geophys. Res.*, **75**, 1766 (1970).
- [15] PRANDTL, L., *Z. Angew. Math. Mech.*, **5**, 136 (1925).
- [16] TCHEN, C. M., «Ph. D. Thesis», Delft, 1947.
- [17] SOO, S. L. and TIEN, C. L., *J. Appl. Mech.*, **27**, 5 (1960).
- [18] ROUHAINEN, P. O. and STACHIEWICZ, J. W., *J. Heat Transfer*, **29 C**, 169 (1970).
- [19] HJELMFELT, A. T. and MOCKROS, L. F., *Appl. Sci. Res., Sect. A*, **16**, 149 (1960).
- [20] RUNSTADLER, P. W., KLINE, S. J. and REYNOLDS, W. C., Thermo Science Division, Dept. Mech. Eng., Rept. MD-8, Stanford University, 1963.
- [21] KIM, H. T., KLINE, S. J. and REYNOLDS, W. C., *J. Fluid Mech.*, **50**, 133 (1971).
- [22] GRASS, A. J., *J. Fluid Mech.*, **50**, 233-255 (1971).
- [23] ECKELMAN, H., *J. Fluid Mech.*, **65**, 439 (1974).
- [24] REICHART, H., M. P. I. für Strommings Furschung Göttingen Dept., No. 6A, 1971.
- [25] ROSENSCHWEIG, R., HATTEL, H. C. and WILLIAMS, *Chem. Eng. Sci.*, **15**, 111 (1961).
- [26] WILLIAMS, I. and HEDLEY, A. B., *Aerosol Sci.*, **3**, 363 (1972).
- [27] WILLIAMS, I., «M. Sc. Thesis», Sheffield, 1970.
- [28] LANGER, G. and RADNIK, J. L., *J. Appl. Phys.*, **32**, 955 (1961).
- [29] DVORAK, K. and SYRED, N., «DISA Conference», Leicester, 1972.
- DVORAK, K. and SYRED, N., Internal Report, Dept. Chem. Eng., University of Sheffield.
- [30] HINZE, J. O., «Turbulence», McGraw Hill, London, 1959, Chap. 2.
- [31] HUGHMARK, E. A., *A. I. Ch. E. (Am. Inst. Chem. Engrs.) J.*, **19**, 1054 (1973).
- [32] MONTGOMERY, T. L. and CORN, M., *Aerosol Sci.*, **1**, 185 (1970).
- [33] SHAW, P. V. and HANRATTY, T. J., *A. I. Ch. E. (Am. Inst. Chem. Engrs.) J.*, **13**, 854 (1974).
- [34] POPOVICH, A. T. and HUMMEL, R. L., *A. I. Ch. E. (Am. Inst. Chem. Engrs.) J.*, **13**, 854 (1974).

## ACKNOWLEDGEMENT

The authors wish to acknowledge the financial and technical assistance of Shell Research Limited which enabled the completion of this work.

## RESUMO

Discutem-se diversas metodologias para o cálculo da velocidade de deposição de partículas sobre as paredes de tubagens percorridas por fluidos em escoamento turbulento. A necessidade de tomar em consideração as relações entre as difusividades turbulentas de massa e de quantidade de movimento é indicada e quantificada experimentalmente. Considerando-se que o escoamento é bidimensional a sua caracterização é feita através dos valores da velocidade média na direcção radial e da raiz quadrada média das flutuações de velocidade na direcção axial, assim como da distribuição da tensão de corte. A partir do último estima-se a difusividade turbulenta do fluido. As medições foram feitas a números de Reynolds de  $1.27 \times 10^5$  e  $2.64 \times 10^4$  sendo a temperatura da parede 294,0 °K. Injectaram-se na corrente fluida gotas de di-2-etilhexilsebacato de diâmetros compreendidos entre 0,54 e 2,6 µm e mediram-se as suas velocidades de deposição, tendo-se observado que esta crescia com o aumento da dimensão da partícula e do número de Reynolds.



The relationship depending upon the type and range of the experimental studies [1]. The flow around a droplet is therefore important in defining these transfer processes, as well as predicting its motion.

The velocity of a droplet may be calculated from a force balance on it

$$\text{Net Force} = \text{Gravity Force} - \text{Bouyancy Force} - \text{Drag Force} \quad (2)$$

The difficulty in the application of the balance arises with the drag force, which is usually expressed in terms of a drag coefficient

$$\text{Drag Force} = \frac{C_d \rho_a V^2 A_p}{2} \quad (3)$$

Many results have been published from studies on the prediction or measurement of drag coefficient and the factors such as drop acceleration, oscillation, distortion, rotation, internal circulation, mass transfer and flow turbulence intensity which effect it [2, 3, 4]. The range of coefficients reported depend upon the flow regime and vary from simple functions of Reynolds number, which may be applied over a wide range with limited accuracy, to more complex relationships, which are more accurate over a limited range. The selection of a suitable one for a particular application may be a compromise between accuracy and the ease of mathematical manipulation.

For use over a range of Reynolds numbers typically encountered in sprays the following coefficient was used with accuracy and convenience [5]

$$C_d = \{23 + (1 + 16\text{Re}^{4/3})^{1/2}\}/\text{Re} \quad (4)$$

for  $1 < \text{Re} < 500$

Equations (1)-(4) enable the history of a spray droplet to be calculated as it passes through a reactor if the properties of the flow surrounding it, characterised by the Reynolds number, are known.

In most applications the droplets are members of polydisperse sprays and from a knowledge of their size distribution [6], it is possible to sum their effect on the overall spray behaviour. There is, however, an interaction between the droplets and between the spray and the surrounding atmosphere, such that the transfer potentials around any individual droplet are uncertain. This uncertainty leads to error in applying single droplet data to the description of sprays.

Interactions between droplets falling in single streams, horizontal assemblages and sprays through liquids have been measured by RAGHAVENDRA and RAO [7]. For this low Reynolds number situation they have found that interaction between droplets in a horizontal plane lead to increased drag while interaction between droplets in a vertical plane resulted in reduced drag and increased terminal velocities. The extent of the deviation was a function of the droplet separation.

ZABEL *et al.* [8] similarly observed a reduction in drag coefficient, of up to 50 %, for drops falling in single streams through stagnant liquids, when compared with single droplet results.

Direct measurements of spray properties have resulted in empirical correlations [9] which are valid for simple sprays, but the variation in droplet sizes and velocities, nozzle types and operating parameters precludes their general use.

More recently attempts have been made to understand these interaction effects for high Reynolds number flows, for liquid sprays in air, in terms of momentum transfer. Observations of the air flow pattern around a hollow cone spray [10] indicated that the flow was induced to enter the spray at right angles to the surface as a result of momentum transfer from the droplets. While passing through the spray the air flow changed to a direction parallel to the nozzle axis and in so doing entrained droplets, moving them into the hollow core. Using such a model, Benatt and EISENKLAM [11] have predicted air entrainment factors for swirl nozzles spraying water into air at ambient conditions. The theoretical and experimental results indicated that entrainment was proportional to spray angle, but there was constantly 25 % difference in the two values over the entire range of results.

From force and momentum balance, across an element of a flat spray BRIFFA and DOMBROWSKI [12]

have predicted air entrainment using a theoretical treatment which requires a knowledge of the drop size distribution and the initial drop velocities. Their results show good agreement with measured flows into iso-octane and tetralin sprays for a wide range of nozzle pressure drops.

To overcome the problems associated with applying single drop theory to sprays an approach based on continuum mechanics was used by ADLER and LYN [13] to predict the steady evaporation and mixing of a liquid spray injected into a gaseous swirl. Some experimental data is however required in order to simplify numerical solution of the differential transfer equations.

These theoretical approaches are all limited in that they describe particular practical situations and do not assess the fundamental processes common to any form of dispersion, or the situations which they describe are complex and do not allow experimental measurement of the parameters which are either theoretically predicted or are empirical constants in the theoretical model.

In this paper the authors describe a more general approach to the problem of assessing interaction effects, by a study of the motion of a single stream of liquid droplets moving at a constant frequency.

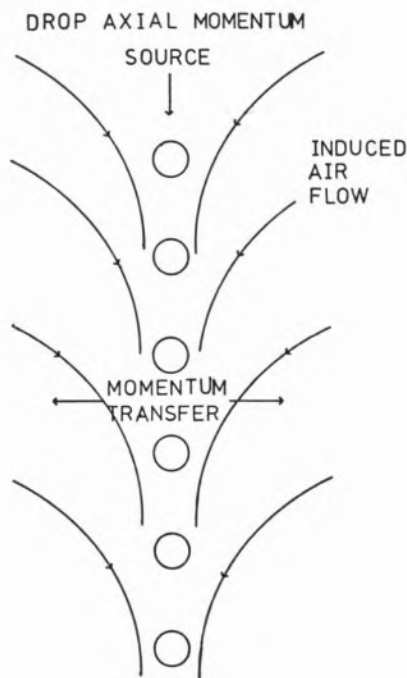


Fig. 1

Drop stream and induced air flows

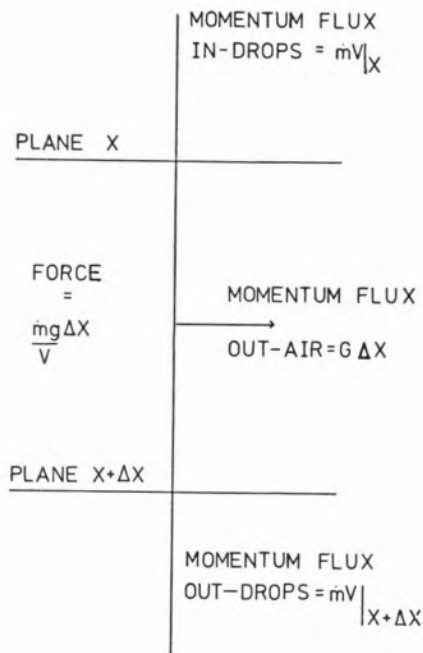


Fig. 2

Force-momentum balance along drop stream axis

The stream constitutes a source of momentum in the ambient fluid, which results in a boundary layer flow being induced around it. The momentum transfer is predicted using a theoretical treatment similar to that of ADLER and LYN [13], and the simplicity of the experimental technique enables accurate measurements to be made for comparison with the theory.

## 2 — THEORY

The theoretical analysis considers the stream of droplets, moving at a constant frequency to be a continuous source of axial momentum with the time averaged properties of the intermittent flow. Momentum is transferred from this source to the surroundings and induces an axisymmetric flow around the stream, fig. 1. The steady laminar flow of a Newtonian fluid within this boundary layer is described by the integral form of the equation of motion

$$\rho_a \frac{\partial}{\partial x} \int_{r=0}^{r=R} r u (u - u(R)) dr = \mu \left[ r \frac{\partial u}{\partial r} \right]_{r=0}^{r=R} \quad (5)$$

The source of x-momentum is related to the viscous shear expression in equation (5) by

$$G = -2\pi\mu \left[ r \frac{\partial u}{\partial r} \right]_{r \rightarrow 0} \quad (6)$$

and  $G$  is given by a force, x-momentum balance, fig. 2

$$G = \left( 1 - \frac{\rho_a}{\rho_p} \right) \frac{\dot{m}g}{V} - \dot{m} \frac{dV}{dx} \quad (7)$$

The axial drop velocity gradient is specified by a force, momentum balance on an individual drop

$$\frac{dV}{dx} = \frac{3C_d\rho_a}{4D_p\rho_p} \frac{(U-V)^2}{V} \frac{(U-V)}{|U-V|} + \frac{g}{V} \left( 1 - \frac{\rho_a}{\rho_p} \right) \quad (8)$$

The radial profile of axial velocity in the boundary layer is assumed to be of the form

$$u(x, \eta) = U(x)F(\eta) \quad (9)$$

where

$$\eta = \frac{r}{b}$$

The integration of the boundary layer equation of motion from the axis to infinity and from the axis to the radius of half maximum air velocity, results in two differential equations which when combined with equation (8) and solved simultaneously enable the drop velocity, air velocity and boundary layer width to be predicted. The approach follows a procedure adopted by SQUIRE and TROUNCER [14].

The numerical integration requires the specification of the initial drop and air stream parameters,  $V(x)$ ,  $U(x)$  and  $b(x)$  at  $x = 0$  and the form of the velocity profile in the boundary layer  $F(\eta)$ .

### 3 — RESULTS

The ability of the theoretical analysis to predict the motion of droplets moving in a stream, through a gaseous or a liquid environments, has been

assessed by comparison with experimental measurements.

Single streams of water droplets, moving at a constant frequency, were produced by the longitudinal vibration of a liquid jet [15]. A droplet was produced during each oscillatory cycle thus producing a time base for measurements of drop velocity. Droplet diameters and interdrop distances were recorded photographically as the drops fell under gravity through a 25 cm long perspex box fitted with optical windows. Drop diameters varied from 250-1250  $\mu\text{m}$ , initial velocities from 1 to 5.5  $\text{ms}^{-1}$  and frequencies from 100 to 5000 drops  $\text{s}^{-1}$ .

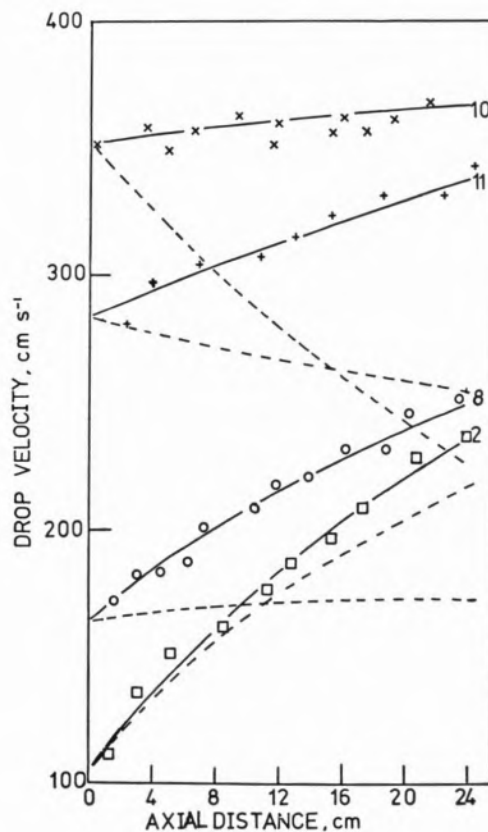


Fig. 3

Measured  $\times + \circ \square$  and predicted stream — and single drop - - - velocities

A comparison between measured stream drop velocities, those predicted by the theoretical analysis from the same initial stream conditions and theoretical predictions for a single drop are shown in fig. 3. The four sets of results cover a range of experimental conditions with increasing deviation

from single drop behaviour. The experimental parameters of these curves are given in Table 1. The curves in fig. 3 illustrate that the stream drop motion is well predicted by the theory when the motion is similar to that of a single drop and also when there is a considerable difference between the motion of a single drop and a stream of drops with the same initial velocity.

To provide further support for the theoretical treatment air velocities were measured in the entrained boundary layer from a hot-wire anemometer traverse. Evidence of the existence of this entrained flow is provided in fig. 4 which shows a titanium tetrachloride smoke tracer emanating from a wire held near to the stream.

Table 1  
Experimental data for fig. 3

Run No.	Initial drop velocity, $\text{ms}^{-1}$	Drop diameter mm	Drop frequency, $\text{s}^{-1}$
2	1.056	1.18	234
8	1.638	0.448	1257
10	3.518	0.380	1736
11	2.827	0.555	1377

The length of the hot-wire anemometer probe used in these measurements was  $1200\ \mu\text{m}$ , somewhat larger than the drop diameter and comparable to the width of the boundary layer. Thus the air velocity was not constant over the length of the wire and the output of the anemometer then represented some mean value interpretation. A theoretical treatment has been developed for the prediction of the radial profile of axial velocity from such a traverse through an axisymmetric flow [16].

An energy balance across the wire gives

$$\frac{d^2T}{dx^2} + Ai^2 + (Bi^2 - C)(T - T_a) - D(T - T_a)f(x)^{\frac{1}{2}} = 0 \quad (10)$$

where ABC and D are constants given by the physical properties of the wire and  $f(x)$  is the

velocity over the wire. The boundary conditions are  $dT/dx = 0$  at  $x = 0$ , the mid-point of the wire and  $T = T_a$  at  $x = 1$ , the end of the wire attached to the probe support. It was assumed that  $f(x)$  could be represented by a parabolic distribution along the wire. Equating the mean temperature of the wire in such a parabolic flow with that from a uniform velocity across the wire enables the mean velocity interpretation in an axisymmetric flow to be converted to a radial velocity profile if the width of the distribution is known.

An example of the non-uniform flow across a wire during a radial traverse is shown in fig. 5 and the transformation of the anemometer readings into a radial velocity profile is shown in fig. 6.

There is a general agreement between measured values of air velocity and boundary layer width and those predicted by the stream entrainment theory. The transformation of anemometer results requires an input conditions for the numerical integration and this is most conveniently provided at present by the maximum air velocity given by a linear approximation analysis of the transformation, reported earlier [17], or by the drop stream velocity. Accepting the limitations of the analysis, which is being further investigated, air velocities agree within  $\pm 10\%$  and boundary layer widths are also comparable.

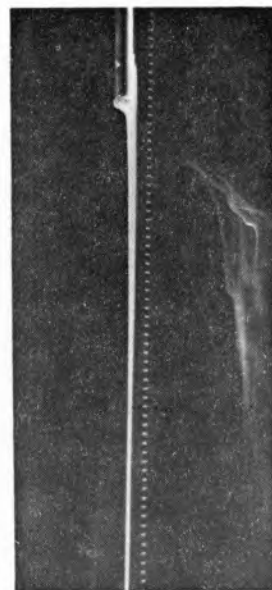


Fig. 4  
Entrainment of a smoke tracer by the drop stream

The results from the studies of the motion of a stream of liquid droplets through air demonstrate the importance of the entrained air flow in predicting droplet trajectories, and provide an explanation for the observed deviations from the standard drag relationships which have been reported by several workers.

The ability of the theory to describe the motion of liquid streams moving through liquids has been assessed by a comparison with the experimental results of other workers.

RAGHAVENDRA and RAO [7] measured the terminal velocities of nitrobenzene drops falling in single streams through water. Drop diameters were varied from 0.2 to 0.6 cm, frequencies from 3 to 4 drops  $s^{-1}$  and measured terminal velocities varied from 9 to 18  $cm\ s^{-1}$ . Terminal stream drop velocities predicted by the theory

$$V_s = \frac{1}{2} (V_t + (V_t^2 + 0.093\ gfD_p^3(\rho_p - \rho_a)/\mu)^{\frac{1}{2}}) \quad (11)$$

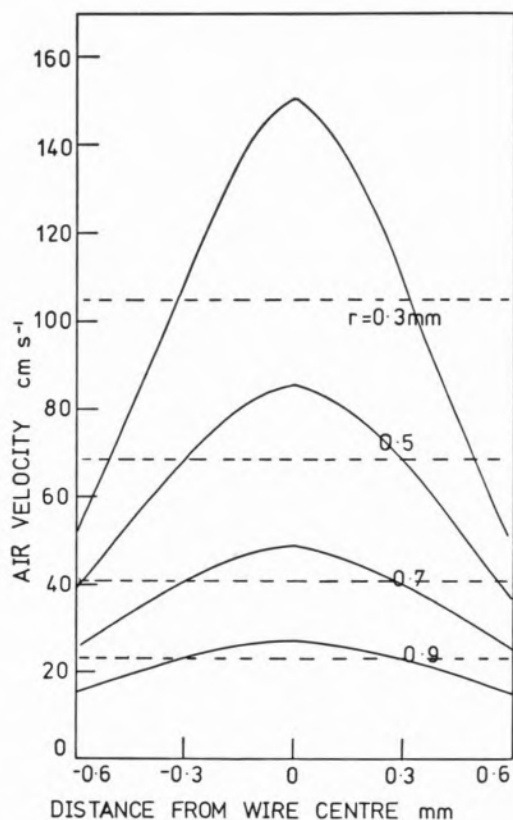


Fig. 5

Variation in velocity distribution along hot-wire with radial position- $r$

are compared with the above experimental results in fig. 7. It is seen that there is an approximate agreement over this narrow range of drop diameters.

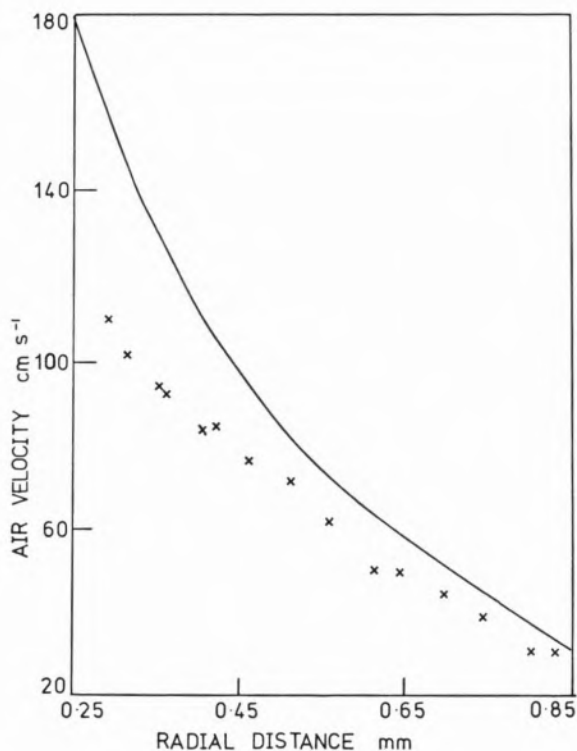


Fig. 6

Transformation of anemometer readings  $\times$  into a radial velocity profile —

The predicted values are based upon a standard curve drag coefficient for solid spheres, equation (4), and cannot take into account the effects caused by drop distortion which occur at Reynolds numbers above 200 [18]. The increased drag which results from the drop distortion is manifested in terms of a reduced terminal velocity over the whole range of drop diameters used in these experiments. Thus although the reduction in drag resulting from stream motion is evident, it is not possible to quantitatively compare the two sets of data.

The reduction in drag coefficient experienced by droplets moving in a stream through a liquid was also measured by ZABEL *et al.* [8]. Cine photography was employed to record the motion of 0.33 cm diameter drops of carbon tetrachloride as they travelled through water-glycerol solutions of various concentrations.

For drops moving at their terminal velocity the drag coefficient is given by

$$C_d = 4(\rho_p - \rho_a)D_p g / 3\rho_a V_t \quad (12)$$

and the drag coefficient for droplets moving in a stream, based on their absolute velocity, can therefore be related to that for a single drop by

$$C_{ds}/C_d = V_t^2/V_s^2 \quad (13)$$

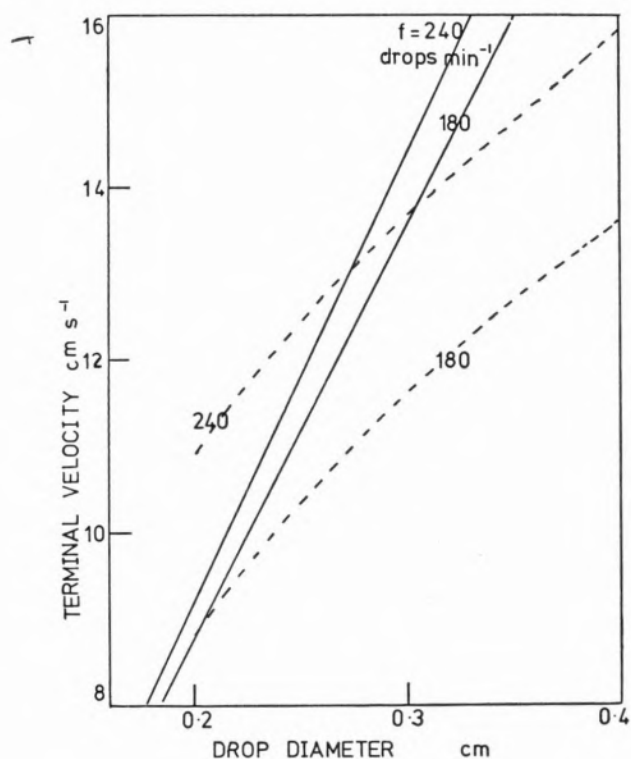


Fig. 7

Predicted — and measured --- drop stream terminal velocities

Equations (11), (12) and (13) can be combined to predict the reduction in drag coefficient experienced by stream droplets

$$C_{ds}/C_d = 4(1 + (1 + 0.07 C_d Re D_p / L)^{1/2})^{-2} \quad (14)$$

and the results compared with the experimental

data of ZABEL *et al.* [8] and RAGHAVENDRA and RAO [7], as shown in fig. 8. It is clear that both experiment and theory demonstrate reduced drag as a result of stream motion, but also that the theory underestimates the effect for  $Re < 150$  and

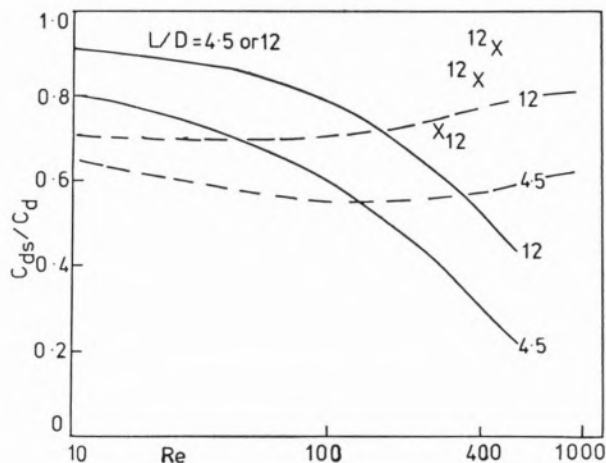


Fig. 8

Reduction of drag coefficient for stream drops, predicted —, measured by Zabel ---, and by Raghavendra x

overestimates for  $Re > 150$ . This closely reflects the comparison of single drop motion with that of a single solid sphere, where at low Reynolds numbers the drag on a sphere is reduced by internal circulation and at higher Reynolds numbers the effects of drop distortion lead to irregular movement and increased drag. These effects appear to be amplified in streams [8].

#### 4 — CONCLUSIONS

The entrainment of the ambient fluid by a stream of drops and the formation of a boundary layer significantly reduces the drag experienced by the droplets and correspondingly increases their terminal velocity. The results imply that the accurate prediction of transport phenomena in dispersed phase systems necessitates the inclusion of terms to account for this flow, and suggests that discrepancies reported between drag data from single particle studies and measurements on spray system may be due to this effect.